Complex ac conductivity of a carbon black composite as a function of frequency, composition, and temperature

D. S. McLachlan*
Physics Department and Condensed Matter Physics Research Unit, University of the Witwatersrand, Johannesburg, South Africa

Michael B. Heaney†
Huladyne Consulting, 160 Waverlye Street, Palo Alto, California 94301-1138

(Received 30 November 1998; revised manuscript received 22 June 1999)

The complex conductivities between 10 mHz and 1 MHz of a series of disordered carbon-black-polymer composites have been measured. The carbon black volume fractions span the percolation threshold, with dc conductivities ranging from 10^{-18} to 10^{-6} $(\Omega\,\mathrm{cm})^{-1}$. The room temperature results are similar to previous measurements on other percolation systems. Conductivity measurements as a function of temperature on a composite sample, slightly above the room-temperature percolation threshold, are consistent with the percolation threshold increasing with temperature and becoming equal to the actual volume fraction at about 130 °C. The real conductivity at different temperatures is shown to scale onto a single curve. An anomalous peak in the real dielectric constant as a function of composition close to the percolation threshold is also observed. [S0163-1829(99)13441-6]

I. INTRODUCTION

The electrical conductivity and dielectric constant, or complex conductivity, of metal-insulator mixtures are the most widely investigated physical properties of percolation systems. Major review articles which include sections on the complex conductivity are Refs. 1–3. Good percolation systems are characterized by a smooth and rapid change of the dc electrical conductivity in a narrow range of conductor volume fractions. It has been well established, both experimentally and theoretically, that near the percolation threshold ϕ_c, the dc conductivity $\sigma(\phi,0)$, ϕ being the volume fraction of conductor, follows the power laws $\sigma(\phi,0)\propto(\phi-\phi_c)^t$ as ϕ_c is approached from the conducting side ($\phi>\phi_c$) with t as the conductivity exponent and $\sigma(\phi,0)\propto(\phi_c-\phi)^{-s}$, where the exponent s describes the divergent behavior of the conductivity, when ϕ_c is approached from the insulating side ($\phi<\phi_c$). The real part of the low-frequency dielectric constant $\varepsilon(\phi,\omega\approx0)$ of percolation systems is also predicted to diverge as $\varepsilon(\phi)\propto|\phi_c-\phi|^{-s}$, where s is the dielectric exponent, on both sides of ϕ_c (Refs. 1–5, and the references therein). A s and a s' are introduced in Refs. 4 and 5 as they are found to be different for the experiments performed on the graphite-boron nitride systems. From early results for computer simulations, model experiments, and some continuum systems, the critical exponents t and s were first thought to be universal, i.e., they depended only on the dimension of the percolation system (which would require $s=s'$, which is not always observed[4,5]) and not on the details of cluster geometry and intergranular contacts. This is now known not to be true for some continuum systems.[1–5]

In analyzing the data the equation used is

$$\frac{(1-\phi)(\phi_i^{1/s}-\phi_m^{1/s})}{(\phi_i^{1/s}+A\phi_m^{1/s})}+\frac{\phi(\sigma_c^{1/t}-\sigma_m^{1/t})}{(\sigma_c^{1/t}+A\sigma_m^{1/t})}=0. \tag{1}$$

This gives a phenomenological relationship between σ_c, σ_i, and σ_m, which are the conductivities of the conducting and insulating component and the mixture of the two components. Note that all three quantities σ_c, σ_i, and σ_m can be real or complex numbers in Eq. (1). The conducting volume fraction ϕ ranges between 0 and 1 with $\phi=0$ characterizing the pure insulator substance ($\sigma_m\equiv\sigma_i$) and $\phi=1$ the pure conductor substance ($\sigma_m\equiv\sigma_c$). The critical volume fraction, or percolation threshold is denoted by ϕ_c, where a transition from an essentially insulating to an essentially conducting medium takes place, and $A=(1-\phi_c)/\phi_c$. For $s=t=1$ the equation is equivalent to the Bruggeman symmetric media equation. Equation (1) yields the two limits

$$|\sigma_c|\to\infty:\quad \sigma_m=\sigma_i\frac{\phi_c^s}{(\phi_c-\phi)^s},\quad \phi<\phi_c, \tag{2}$$

$$|\sigma_i|\to0:\quad \sigma_m=\sigma_i\frac{(\phi-\phi_c)^t}{(1-\phi_c)^t},\quad \phi>\phi_c \tag{3}$$

which characterize the exponents s and t. Note that Eqs. (2) and (3) are the normalized percolation equations. In the crossover region where ϕ lies between $\phi_c-(\sigma_i/\sigma_c)^{1/(s+t)}$ and $\phi_c+(\sigma_i/\sigma_c)^{1/s+t}$,[1–3]

$$\sigma_m\approx\sigma_i^{s/(s+t)}\sigma_c^{t/(s+t)}. \tag{4}$$

The scaling conditions used in this paper, which are based on those given in Refs. 1–3, are

$$\sigma_m=\begin{cases}\sigma_c\dfrac{(\phi_c-\phi)^t}{\phi_c^t}F_-(x_-), & \phi<\phi_c \quad (5)\\ \sigma_c\dfrac{(\phi-\phi_c)^t}{(1-\phi_c)^t}F_+(x_+), & \phi>\phi_c, \quad (6)\end{cases}$$

where σ_m can be the theoretical result from Eq. (1) or the experimental results. The scaling functions $F_{\pm}(x_{\pm})$ depend on the scaling parameters,

$$x_- = \frac{\sigma_i}{\sigma_c}\frac{\phi_c^{s+t}}{(\phi_c-\phi)^{s+t}} = -i\frac{\omega}{\omega_{c-}}, \quad \phi<\phi_c \tag{7}$$

with

$$\omega_{c-} = \frac{\sigma_c}{\varepsilon_0\varepsilon_i}\frac{(\phi_c-\phi)^{s+t}}{\phi_c^{s+t}}$$

and

$$x_+ = \frac{\sigma_i}{\sigma_c}\frac{(1-\phi_c)^{s+t}}{(\phi-\phi_c)^{s+t}} = -i\frac{\omega}{\omega_{c+}}, \quad \phi>\phi_c \tag{8}$$

with

$$\omega_{c+} = \frac{\sigma_c}{\varepsilon_0\varepsilon_i}\frac{(\phi-\phi_c)^{s+t}}{(1-\phi_c)^{s+t}} \quad [\alpha\sigma_m(\phi,0)^{[(s+t)/t]}].$$

The above expressions for $\omega_{c\pm}$ assume a purely real $\sigma_c(\sigma_{ci}=0)$ and imaginary $\sigma_i(\sigma_{ii}=-\omega\varepsilon_0\varepsilon_I, \sigma_{ir}=0)$, as was done in Refs. 1–3, 6. However, it is stressed that all results obtained in this section are independent of whether the conductances and hence the scaling functions $F_{\pm}$ are genuinely complex or real. To ensure that curves drawn for $F_{\pm}$ fall on top of each other for different ϕ_c, the normalization employed in all the equations used in this paper differs somewhat from the one used in Refs. 1–3.

As ω is varied, the $F_+(x_+=i\omega/\omega_{c+})$ and $F_-(x_-=i\omega/\omega_{c-})$ curves with different σ_i/σ_c, ω/ω_{c+}, and ω/ω_{c-} values, but with compensatory changes in ϕ or ϕ_c such as to give the same x_+ and ω/ω_{c+} or x_- and ω/ω_{c-} values, superimpose for the same t and s values.[8,9] It can be shown,[7–9] that the limiting slopes of F_+ and F_- against x_+, x_-, ω/ω_{c+} and ω/ω_{c-} are

$$\mathrm{Re}\,F_+(x_+) \ [\text{and } \mathrm{Re}\,F_+(-i\omega/\omega_{c+})] = 1 \quad (\text{for } x_+ \text{ or } \omega/\omega_+<1), \tag{9a}$$

$$\mathrm{Im}\,F_-(x_-) \ [\text{and } \mathrm{Im}\,F_-(-i\omega/\omega_c)] = x_-(\omega/\omega_{c-}) \quad (\text{for } x \text{ or } \omega/\omega_c<1), \tag{9b}$$

$$F_+(x_+) \ [\text{and } F_+(-i\omega/\omega_{c+})] \propto x_+^{t/(s+t)}((\omega/\omega_{c+})^{t/(s+t)}) \quad (\text{for } x_+ \text{ or } \omega/\omega_{c+}>1), \tag{9c}$$

$$F_-(x_-) \ [\text{and } F_-(-i\omega/\omega_c)] \propto x_-^{t/(s+t)}((\omega/\omega_{c-})^{t/(s+t)}) \quad (\text{for } x_- \text{ or } \omega/\omega_{c-}>1). \tag{9d}$$

All of these limits, including both the real and imaginary components of F_+ and F_- in Eqs. (9c) and (9d), which are derived analytically in Ref. 8 and shown numerically in Refs. 7–9, are the same as for the scaling functions defined in Refs. 1–3. However, the second-order terms of the complex functions F_+ (i.e., $\mathrm{Im}\,F_+$) and F_- (i.e., $\mathrm{Re}\,F_-$) [or $\sigma_{mi}(\phi>\phi_c)$ and $\sigma_{mr}(\phi<\phi_c)$] differ from those in Eqs. (9a) and (9b) when $x_+(\omega/\omega_{c+})<1$ and $x_-(\omega/\omega_{c-})<1$. This has been shown analytically in Ref. 8, where measurements of $\sigma_{mi}(\phi>\phi_c)$ and $\sigma_{mr}(\phi<\phi_c)$, which help to resolve this dilemma, have also been reported. Recall that for $x_+(\omega/\omega_+)>1$ and $x_-(\omega/\omega_-)>1$ there is agreement between Eqs. (9c) and (9d) and the equations given in Refs. 1–3, and 6 for both first- and second-order terms. The previously defined crossover region now corresponds to x_+ and $x_->1$.

Unfortunately, analytic solutions to the complex equations for $F_+(x_+)$ and $F_-(x_-)$ are not available for arbitrary s and t. However, with the values of $s=1$ and $t=2$ or $t/s=2$, $F_+(x_+)$ and $F_-(x_-)$ can be calculated from a complex cubic equation.[8] Any t/s value equal to an integer gives a polynomial equation, which can then be solved.[8] For arbitary t/s Eq. (1) can be solved numerically. Note that Eq. (1) can be solved as an implicit equation for arbitrary s and t if σ_c and σ_i are real.[9] This approach, using Eqs. (5)–(8), was successfully used to fit the scaled data, $\sigma_r(\phi>\phi_c)$ and $\sigma_i(\phi<\phi_c)$, for the graphite-boron nitride system.[7]

In this paper we report on the experimental studies of the complex ac conductivity (dielectric constant) of carbon black–polyethylene percolation composites. Composites of this type are manufactured by several different companies and marketed in the form of resetable fuses and self-regulating heaters.[10] Three compositions below ϕ_c, with nominal CB compositions of 0, 12, and 17 % and two above ϕ_c, nominal (and actual) compositions 17.5% (0.1789) and 18.65% (0.1885) CB were measured at room temperature. The 17.0% sample was very close to the percolation threshold ϕ_c at room temperature. The 17.5% sample was measured between 27 and 134 °C (note the melting point of the polymer is about 130 °C). The real conductivity decreases as the temperature increases as ϕ and φ_c increase but $\varphi-\varphi_c$ decreases.[19] It will be shown that the conductivity results can, to a good approximation, be scaled onto a single curve using the procedures outlined above. A behavior, inconsistent with the predictions of Refs. 1–3, is observed for the dielectric constant measured when $\varphi \gtrsim \varphi_c$ in that it increases with $\varphi-\varphi_c$, whereas it should decrease as $(\varphi-\varphi_c)^{-s}$.[1–3] Solutions of Eq. (1) show dielectric terms that continue to increase with φ above φ_c, reaching a maximum somewhat above φ_c.[8]

In the remainder of the paper, the experimental procedures are described in Sec. II. The experimental data are the discussion and analysis of the data are presented in Sec. III. A summary of the results and the conclusions made are given in Sec. IV.

II. EXPERIMENTAL METHODS

The samples are composed of commercial carbon black and polymer and have been described before.[11] The carbon black resistivity is of order $10^{-2}\,\Omega$ cm and the polymer resistivity about $10^{18}\,\Omega$ cm. The carbon black consists of 200 nm mean diameter aggregates composed of smaller fused semispherical particles of 80 nm mean diameter. Carbon black aggregates are known to form larger agglomerates when melt compounded with a polymer. The largest structures visible in a transmission electron micrograph which

may be agglomerates are about 1 μm in diameter.[12] The polymer is high-density polyethylene with a melting point of 130 °C. The preweighed carbon black and powdered polymer are mechanically mixed and then melt compounded in a Moriyama batch mixer at 150 °C. Each compound is compression molded into three slabs of nominal thickness 0.025 cm and then cut into samples of nominal width 1.25 cm and nominal length 18 cm. The concentration of carbon black in the composite is determined by thermogravimetric analysis of four pieces near the edges of the three slabs.[11]

Before applying the electrical contact, the surfaces of the samples were lightly sanded using 220 grit emery paper. Strips about 180 mm long, 12.5 mm wide, and 0.2 mm thick were used for the more conducting samples and sheets up to 180×100 mm were available for the samples below φ_c. Where needed, four resistivity contacts were made by painting silver current contacts onto the ends and voltage contacts about 50 mm from the middle of the appropriate strip sample. This configuration was used for dc conductivity measurements, but two probe ac conductivity measurements had to be made with the Novocontrol Dielectric Spectrometer. The low-frequency ac and dc resistivities agreed with each other within a few percent, indicating negligible current contact resistance. (In a trial experiment it was found that the values of capacitances, made on 17.5% material, did not change when gold was first sputtered below the silver paste capacitor plates.) The capacitor areas were chosen so that the capacitance and resistance of the sample were, where possible, well within the measurement limitations (capacitance, resistance, and tan δ) of the Dielectric Spectrometer.

The Novocontrol Dielectric Spectrometer is an instrument especially designed for measurements of this nature. This instrument, working from the subhertz to megahertz range, is capable of measuring far smaller loss components in the dielectric or insulating phase (equivalent to $10^{14}\,\Omega$ at 10^{-2} Hz and $10^{8}\,\Omega$ at 10^{5} Hz in parallel with an ideal capacitor) and has a better resolution of loss or phase angle (a maximum of tan δ of $>10^{3}$ and a minimum of 10^{-3}) than the instruments used in Refs. 4 and 5 or any previous measurements of a similar nature.[13–18]

The measurements were done in a copper chamber to which was attached a 120 W heater. The samples, coaxial lead terminations, a thermocouple, and a PT100 platinum resistance thermometer were all mounted on a Teflon plate in the middle of the chamber. The temperature was controlled, with air as the exchange medium, using the PT100 resistance and Lake Shore DRC/93CA temperature controller. A stability during the measurements of plus or minus 0.2 °C was achieved during measurements, as determined from the temperature controller and a thermocouple.

III. RESULTS AND DISCUSSION

Extensive room-temperature dc conductivity measurements have previously been made on the samples described above and other samples in this series.[11] The important results from this paper are that $t=2.9\pm0.1$ and that $0.1676<\varphi_c<0.1789$ for this system. As s has not been measured for this system, one can only assume a value of between about 0.5 to 0.9 from other ac dielectric measurements,[4,5,13–18] the universal value being 0.87 or even 1 for ease of computing.

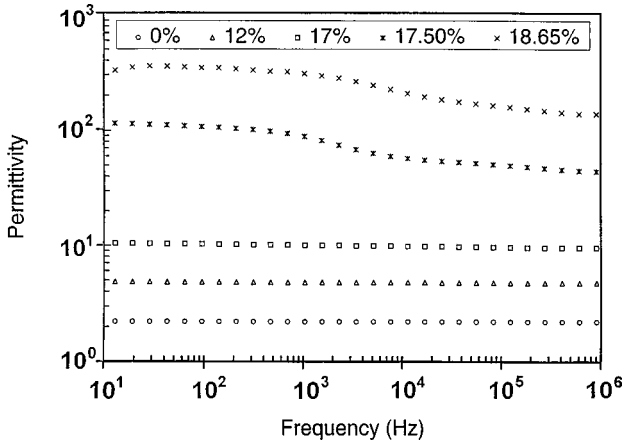

FIG. 1. Experimental values of the permittivity (ε_{mr}) are plotted against frequency at room temperature for all the carbon volume concentrations.

Figures 1 and 2 give the real relative dielectric constant and conductivity for the 0, 12, 17, 17.5, and 18.65 % samples at room temperature, as a function of frequency. The dielectric measurements are only shown down to 10 Hz, as some of the results became erratic below this frequency. Comparing these results with the various limiting slopes given above and in Refs. 1–3 and with the experimental results given in Refs. 7 and 13–18, one can conclude from the dispersion free dielectric constants and the power-law dispersion of the conductivity of the 0, 12, and 17 % samples, that these samples are insulating. However, the slopes for the conductivity of the 12 and 17 % samples are almost exactly 1 and not 2 as is to be expected from Refs. 1–3. Note that there must be a real dielectric conductivity or loss term in the polyethylene itself, which, from Fig. 2, has a power law of about $\omega^{0.9}$ from the 0% sample. This loss must also be a major contributor to the conductivity observed in the 12 and 17 % samples. The dielectric loss term, as it appears in Eqs. (1), (5), and (6), is discussed in more detail, with $\varepsilon_i^*=\varepsilon_{ri}+\varepsilon_{ii}(\omega)$, in Ref. 8. From the shape of the conductivity curves in Fig. 2 the 17.5 and 18.65% samples are clearly

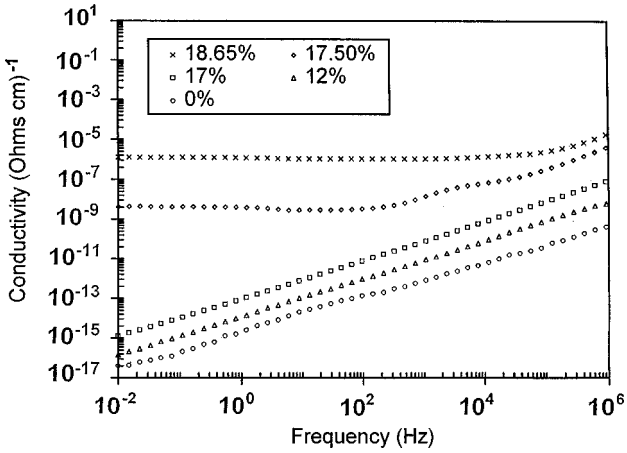

FIG. 2. Experimental values of the conductivity (σ_{mr}) are plotted against frequency at room temperature for all the carbon volume concentrations.

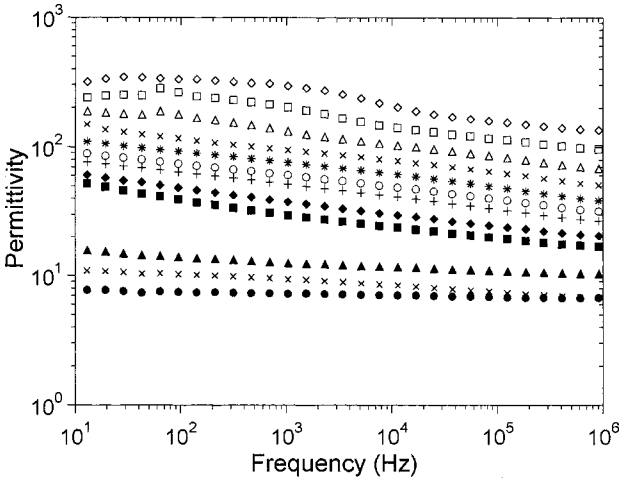

FIG. 3. Experimental values of the permittivity (ε_{mr}), are plotted against frequency for the 17.5% sample at various temperatures. [27.1 °C (◇), 80 °C (□), 100 °C (△), 110 °C (×), 115 °C, (∗), 118 °C (○), 120 °C (†), 122 °C (♦), 126 °C (■), 128 °C (▲), 130 °C (●), 134 °C (×)].

conducting. The permittivity data, as a function of frequency, for these two conducting samples are not understood, but very few data of this nature exist in the literature. However, the dielectric constants of these two samples are increasing with φ above φ_c (i.e., $\varphi-\varphi_c$) for all frequencies, in clear contradiction with the $(\varphi-\varphi_c)^{-s}$ dependence predicted in Refs. 1–3.

Figures 3 and 4 show the real dielectric constant and conductivity as a function of frequency, for the 17.5% sample in the temperature range 27.1–134 °C. From the shape of the conductivity curves the sample below 130 °C have $\varphi>\varphi_c$, but the decrease in conductivity with temperature shows $(\varphi-\varphi_c)$ is decreasing with temperature. This is to be expected as φ_c increases more rapidly than ϕ with temperature.[19] The origin of the slow oscillations in the low-frequency data is not known. Note that the dielectric constant above φ_c (134 °C) is again increasing with $(\varphi-\varphi_c)$, as it did in Fig. 1.

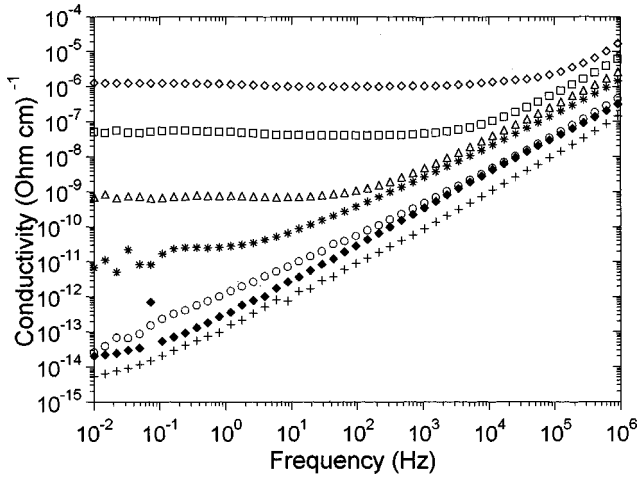

FIG. 4. Experimental values of the conductivity (σ_{mr}), are plotted against frequency for the 17.5% sample at various temperatures. [21.1 °C (◇), 110 °C (□), 120 °C (△), 126 °C (∗), 128 °C (○), 130 °C (+), 134 °C (♦). The 80, 100, 115, 118, 122, and 126 °C plots have been omitted for clarity.]

The slope of the 122 °C curve (where $\phi>\phi_c$) at high frequencies is 0.94, somewhat higher than is to be expected. [Note $t/(s+t)=2.9/(0.5+2.9)=0.85$, with $s=0.5$, this being a reasonable minimum value.] The dielectric constant decreases with frequency. At the lower temperatures the dielectric dispersion curve is not a simple power law but evolves into a power law as the temperature increases. At 122 °C there is a power-law dependence of -0.1 ($s/s+t=0.15$ with $t=2.9$ and $s=0.5$). According to Refs. 1–3 these results for ε_{mr} should show no dispersion. Note that as Fig. 4 clearly shows the sample to be conducting, the 122 °C sample is not in the crossover region (ω/ω_{c+} and $\omega/\omega_{c-}>1$) where Eqs. (9c) and (9d) are obeyed.

An alternative interpretation for the above exponents is that these composites are exhibiting mean-field behavior in their ac electrical properties. This interpretation is consistent with earlier experiments on the dc electrical properties of these same composites,[11] which also found critical exponents in excellent agreement with the predictions of mean-field theory. The values for the critical exponents for mean-field theory are identically the Bethe lattice values. Using the mean-field values in the intercluster polarization model gives $t/(s+t)=1$. Using the mean-field values in the anomalous diffusion model also gives $t/(s+t)=1$. These theoretical mean-field values are in very good agreement with the experimental values for $t/(s+t)<1$ [and $s/(s+t)\approx 0$] measured in this paper. These theoretical mean-field values are also in excellent agreement with the experimental value $t/(s+t)=1\pm 0.05$ measured in percolative gold films at room temperature in the intermediate frequency regime by Hundley and Zettl.[18]

The metal insulator transition occurs at about 130 °C, the exact value depending on ϕ.[17] Therefore at and near 130 °C, one might expect the sample to be in the crossover region where Eqs. (9a) and (9b) should be obeyed. The slopes of the 128, 130, and 134 °C conductivity curves in Fig. 4 are at first sight consistent with this, except for the fact that all the slopes are again much closer to 1 than the expected value of about 0.85. Note too that all three dielectric constants are nearly dispersion free, whereas they should have a slope of $-s/(s+t)$, with a reasonable minimum of $0.5/(0.5+2.9)=0.147$, if they were in the crossover region. Therefore, it would appear that these samples must be classified as insulating and that the temperature range where crossover behavior could be observed must be very narrow. dc scaling also suggests a very narrow crossover regime.[11] The increase in the real dielectric constant and conductivity for the sample at 134 °C, above those at 130 °C, is almost certainly due to the sample having melted. Samples recovered from this temperature were always severely distorted. (Note that as these samples are not radiation crosslinked, they will flow above melting point.)

As the conductivity data curves are qualitatively similar to what has been observed before it is interesting to see if the curves can be scaled as in Refs. 5 and 7. First an $F_+(\omega/\omega_c)$ curve was calculated, using Eqs. (1), (5), and (6), with $s=0.5$ and $t=2.9$ to get the reasonable maximum slope (0.85). The other values used were $\sigma_c=6666\,\Omega^{-1}\,\mathrm{m}^{-1}$,[11] 2.1 ($\varepsilon_r$ from Fig. 1) $x\varepsilon_0 x\omega$, and $\varphi_c=0.17$,[11] ω and φ being varied over a sufficient range to generate a overlapping F_+, as was done in Refs. 7 and 9. To obtain the experimental

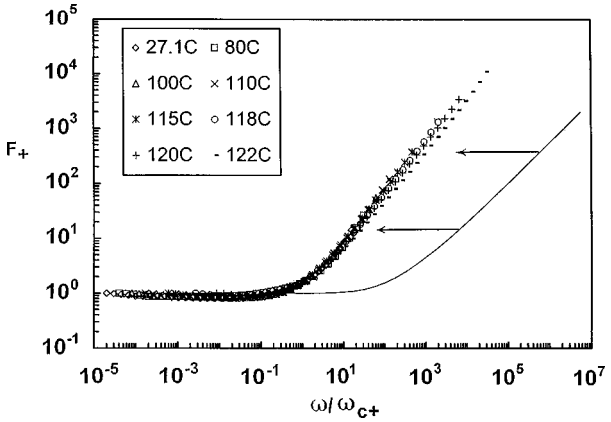

FIG. 5. The scaled conductivities $\sigma_{mr}(\varphi,\omega)/\sigma_m(\varphi,0)$ plotted against the log of the scaled frequency ω/ω_{c+} for the 17.5% sample at various temperatures. The origin of the F_+ plot shown, displaced to the right in the figure, is discussed in the text.

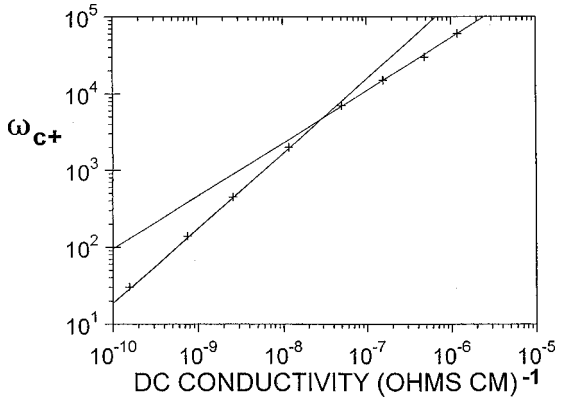

FIG. 6. The experimental values of ω_{c+} are plotted against the measured dc conductivity.

points the results for the conductivity data at and below 122 °C, shown in Fig. 3, were first divided by the conductivity at the lowest frequencies (which is very close to the measured dc value). The resulting curves were then slid along the $\ln[\sigma_{mr}(\varphi,\omega)/\sigma_{mr}(\varphi,0)]=0$ axis, by a scaling factor $1/\omega_c$(expt), until the experimental curve coincided with the calculated F_+ at $\omega/\omega_c=1$. The experimental results and F_+ are shown in Fig. 5. Note that the experimental curves do not overlap particularly well and certainly not as well as those given in Refs. 5 and 7. Note too that the limiting slope for large ω/ω_+ decreases with temperature but is always larger than one which is in conflict with Refs. 1–3 and 6 and other experimental results.[5,7,13–18]

The present experimental system differs from those discussed in Refs. 5, 7, and 13–18 as in a CB-polymer system some or all of the grains may be wet and continuously coated by the insulator (polymer). This is not the case for the systems discussed in Refs. 5, 7, and 13–18. However, work done over an extremely large frequency range on another class of carbon black polymer samples,[20] gives values for the high-frequency slopes of log conductivity versus log frequency graphs that are less than 1. This shows that the behavior of different carbon black–polymer systems are not necessarily the same. Indeed the electron transport method mechanism in conductor-polymer composites is still in serious dispute (Ref. 21, and references therein).

In spite of this only semiquantitative agreement with the predictions of scaling, a plot of $\ln\omega_c$ against $\ln\sigma_{mr}(\varphi,0)$ was made and is given in Fig. 6. Note that at the highest temperatures a straight line with slope 0.925 is obtained. Note too that Eq. (8) predicts that the slope should be $q=(s+t)/t$, which is always greater than 1. Experimental results[5,6,15,17,18] give slopes both greater and less than 1 but always less than the value of q expected from the measured values of s, t, and or $t/(s+t)$. Note too that the value of ω_c(calc) calculated from Eq. (8) at 27.1 °C, where $\phi-\phi_c$ is known, with the exponents given above is many orders of magnitude greater than ω_c(expt). Widely different values of ω_c(calc) and ω_c(expt) has been noted in Ref. 22 and discussed in Ref. 7. The even lower slope obtained at lower temperatures is not understood.

The smooth increase in ε_r with φ up to and beyond φ_c can be clearly seen in Fig. 1, while Fig. 3, where $\phi>\phi_c$ for $T>130$ °C, shows ε_r increases with $(\varphi-\varphi_c)$, being a maximum at the lowest temperature. While the behavior of ε_r shown in Fig. 3 has not been emphasized in previous work, it is consistent with the behavior of ε_r shown in Fig. 1. The smooth increase in ε_r with φ beyond φ_c has recently been seen in graphite-boron nitride[8] and a number of systems where fine conducting powders are impregnated on the surface of larger almost spherical grains, before the grains are compressed into a three-dimensional continuum.[23] This phenomenon has also been seen before for Al spheres in epoxy resin[24] and probably many other systems. Attention was probably not called to, nor paid to these and other similar results, as they are in conflict with standard percolation theory as given in Refs. 1–3.

Figure 7 shows the experimental ε_r results between $\varphi=0.15$ and 0.19 at 1 kHz and calculations made using Eq. (1) with $\varphi_c=0.172$, $\sigma_c=6666\,(\Omega\,\mathrm{m})^{-1}$, $\varepsilon_{ri}=2.1$, $t=3.0$, and $s=0.6$ (dashed lines) and 1.0 (solid lines) at 1 kHz. (the more peaked curve) and 1 MHz. These parameters, except for s, all were obtained from previous measurements.[11] Similar results for graphite-boron nitride and NbC coated insulating grains together with more details of the computational procedures are given in Ref. 8.

It is obvious that the fit is at best qualitative. Better fits can be obtained if the parameters are varied, for instance, increasing φ_c, which will obviously move the plots to the

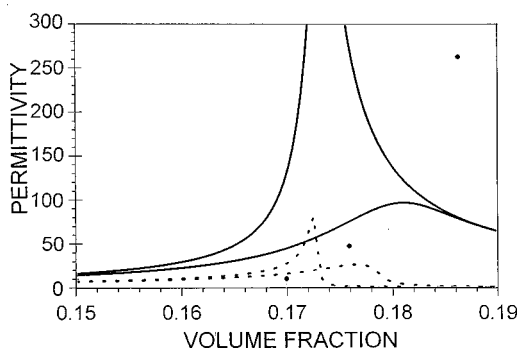

FIG. 7. Experimental values of the permittivity (ε_{mr}) for the 17, 17.5, and 18.65 % samples, at room temperature and 1 kHz, plotted against the volume fraction (φ). The nature of the theoretical curves and the parameters used are given in the text.

right. Theoretical plots for various combinations show that the peaks, at a fixed frequency, broaden and the peak height drops if $i\omega\varepsilon_0\varepsilon_r/\sigma_c$ decreases and s and/or t is increased. This combines to indicate that this ''hump'' occurs in the crossover region [i.e., the region between where $\sigma_{rm}\propto(\varphi-\varphi_c)^t$ and $\varepsilon_{rm}\propto(\varphi_c-\varphi)^{-s}$ hold], the width to which it is proportional $(\omega\varepsilon_0\varepsilon_r/\sigma_c)^{(1/s+t)}$, also broadens. This seems intuitively correct to the authors as in the crossover region, the properties of both components play nearly equal roles in determining σ_m or ε_m. For $\phi\gg\phi_c$, Eq. (1) predicts that $\sigma_{mi}\propto\omega^{1/s}$ and $\varepsilon_{mr}\propto\omega^{(1-s)/s}$.[8]

IV. SUMMARY AND CONCLUSIONS

The conductivity data shown in Fig. 1 clearly show that the 0, 12 and 17 % samples are below the percolation threshold while the 17.50 and 18.65 % ones are above. This agrees with the range of $\varphi_c s(0.1676-0.1789)$ given in Ref. 11. The ω dependence observed for the insulating samples is in line with those seen in most previous work.[7,13–18] The σ_{mr} lines are fairly parallel to the pure polyethylene sample (0%) and as pointed out in Ref. 8 the other two lines are probably dominated by the percolation enhanced polyethylene loss. The dielectric constant of the insulating samples is consistent with percolation theory[1–3] but that of the conducting samples is not, neither as a function of frequency or φ. Equation (1) does allow for an increase in ε_{mr} above φ_c, but is certainly not quantitatively correct using previously measured parameters.

The changes in the conductivity with temperature, shown in Fig. 4, are consistent with the model that the sample is approaching the insulating state (i.e., $\varphi_c>\varphi$) at 134 °C, as φ_c increases with temperature faster than φ. From the conductivity data it is not certain if the insulating state is reached but the almost complete lack of dispersion in the 134 °C samples shows that this is probably the case. The permittivity data in Fig. 3 decreases with temperature, consistent with the data in Fig. 1 and a decrease in $(\varphi-\varphi_c)$ with temperature.

The conductivity data can be scaled as described in the theory section and done in Ref. 7. However, the slopes observed in the crossover region $(\omega/\omega_{c+}>1)$ are greater than 1 whereas the maximum value, according to percolation theory and Eqs. (9a) and (9b), must be less than 1 (or $t/s+t$). It is therefore somewhat of a surprise that ω_c plotted against the dc conductivity gives a straight line at the higher temperatures, where linear ε_r against frequency plots are obtained. The value for q is consistent with previous experiments but not theory. The only conclusion is that scaling is a very universal phenomenon, but our ability to understand it is still limited.

The smooth increase in ε_r with φ above φ_c is at first sight surprising, but it is found to also have been observed in a number of different systems, with both a polymer and nonpolymer insulating component. An explanation must be sought. This will certainly not come from percolation theory as given in Refs. 1–3. Equation (1) provides, at best, only a qualitative model for the data in Fig. 7 unless parameters (σ_c, σ_i, φ_c, s, and t) very different from those measured in a function of φ experiments are used. An explanation of this phenomenon obviously requires further thought, modeling, and experimentation.

ACKNOWLEDGMENTS

The authors would like to express their appreciation for the hard and enthusiastic work that their two vacation students, Ivan Stegic and Robert Ambrosi, put into taking and plotting the data.

*Electronic address: mclachlan@physnet.phys.wits.ac.za
†Electronic address: mheaney@alum.mit.edu

[1] J. P. Clerc, G. Girand, J. M. Langier, and J. M. Luck, Adv. Phys. **39**, 191 (1990).
[2] D. J. Bergman and D. Stroud, in *Solid State Physics*, edited by H. Ehrenreich and D. Turnbull (Academic, San Diego, 1992), Vol. 46, p. 147.
[3] Ce-Wen Nan, Prog. Mater. Sci. **37**, 1 (1993).
[4] Jungie Wu and D. S. McLachlan, Phys. Rev. B **56**, 1236 (1997).
[5] Jungie Wu, Ph.D. thesis, University of the Witwatersrand, 1997.
[6] A. L. Efros. and B. I. Shklovskii., Phys. Status Solidi B **76**, 475 (1976).
[7] Jungie Wu and D. S. McLachlan, Phys. Rev. B **58**, 14 880 (1998).
[8] D. S. McLachlan, W. D. Heiss, C. Chiteme, and Jungie Wu, Phys. Rev. B **58**, 13 558 (1998).
[9] D. S. McLachlan, Physica B **254**, 249 (1998).
[10] F. A. Doljack, IEEE Trans. Compon., Hybrids, Manuf. Technol. **CHMT-4**, 372 (1981); J. A. Oakes and C. L. Sandberg, IEEE Trans. Ind. Appl. **IA-9**, 462 (1973).
[11] M. B. Heaney, Phys. Rev. B **52**, 12 477 (1995).
[12] M. B. Heaney, Physica A **241**, 296 (1997).
[13] Y. Song, T. W. Noh, S. I. Lee, and J. R. Gaines, Phys. Rev. B **33**, 904 (1986).
[14] I. G. Chen and W. B. Johnson, J. Mater. Sci. **26**, 1565 (1991).
[15] L. Benguigui, J. Phys. Lett. (France) **46**, L-1015 (1985).
[16] R. B. Laibowitz and Y. Gefen, Phys. Rev. Lett. **53**, 380 (1984).
[17] R. K. Chakrabarty, K. K. Bardhan, and A. Basu, J. Phys.: Condens. Matter **5**, 2377 (1993).
[18] M. F. Hundley and A. Zettl, Phys. Rev. B **38**, 10 290 (1988).
[19] M. B. Heaney and H. Pan (unpublished).
[20] L. J. Adriaanse, J. A. Reedijk, P. A. A. Teunissen, H. B. Brom, M. A. J. Michels, and J. C. M. Brokken-Zijp, Phys. Rev. Lett. **78**, 1755 (1997).
[21] M. B. Heaney, Appl. Phys. Lett. **69**, 2602 (1996).
[22] A. Sarychev and F. Brouers, Phys. Rev. Lett. **73**, 2895 (1994).
[23] C. Chiteme and D. S. McLachlan, in *Electrically Based Microstructural Characterization II*, edited by R. A. Gerhardt, M. A. Alim, and S. R. Taylor, MRS Symposia Proceedings No. 500 (Materials Research Society, Pittsburgh, 1998), p. 357; (private communication).
[24] L. Layeychine and F. Carmona (private communication).